Applied Mathematical Modelling 40 (2016) 2661–2673

Contents lists available at ScienceDirect

Applied Mathematical Modelling

journal homepage: www.elsevier.com/locate/apm

Multidimensional wave fronts propagation along the beams associated with thermodynamic model of a rotating detonation engine

Ranis N. Ibragimov*

GE Global Research, 1 Research Circle, Niskayuna, NY 12309, USA

ARTICLE INFO

Article history:
Received 20 February 2015
Revised 14 August 2015
Accepted 23 September 2015
Available online 20 October 2015

Keywords:
Rotating detonation engines
Wave fronts

ABSTRACT

The main purpose here is to develop an analytic approach for investigating the wave front propagation on a surface of a cylinder that can be used as a descriptor of a detonation engine. The analysis is based on a weakly nonlinear approximated gas dynamic equations with incorporated approximation of the Korobeinikov's chemical reaction model that are used to describe the two-dimensional detonation field on a surface of a two-dimensional cylindrical chamber without thickness. We found that the wave fronts can be expressed analytically in explicit form for special classes of flow (e.g. isentropic gas flow). In more general cases, the dynamics of wave fronts can still be determined explicitly provided that the wave front is known at initial time and the exact solution is either known a priori, e.g. from experimental or numerical analysis.

1. Introduction

Within the last 15 years, there has been a considerable amount of research into developing engines utilizing detonation waves for air-breathing propulsion, to the point where propulsion engines are being developed and tested [1,2].

Rotating detonation engine (RDE) takes a different approach toward realizing the efficiency of the detonation cycle [3]. By allowing the detonation to propagate azimuthally around an annular combustion chamber, the kinetic energy of the inflow can be held to a relatively low value, and thus RDE can use most of the compression for gains in efficiency, while the flow field matches the steady detonation cycle closely [4].

A basic mechanism of RDE is shown in Fig. 1. The micro-nozzles flow in a premixture of fuel and air or oxygen, and a detonation propagates circumferentially around the combustion chamber consuming the freshly injected mixture. The gas then expands azimuthally and axially, and is either subsonic or supersonic (or both), depending on the back pressure at the outlet plane. Similarly to our previous studies in [5], where the dynamics of small perturbations of a certain class of stationary exact solutions to the nonlinear governing equations of geophysical stratified fluid motion in a cylindrical wave field was investigated, the flow in RDE has a very strong circumferential aspect [6]. However, unlike in [5], in which such a flow was in virtue of stratification and the effects of rotation due to the Coriolis force, for RDE, a such circumferential aspect is due to detonation wave propagation [7].

Similar to our approach in [5], since for RDE, the radial dimension is typically small compared to the azimuthal and axial dimension, we shall neglect the radial dependence in our modeling, which allows the RDE to be unrolled into two dimensional

* Tel.: +1 9562031382.
E-mail address: Ranis.Ibragimov@ge.com, ibrranis@gmail.com

http://dx.doi.org/10.1016/j.apm.2015.09.027
S0307-904X(15)00561-2/

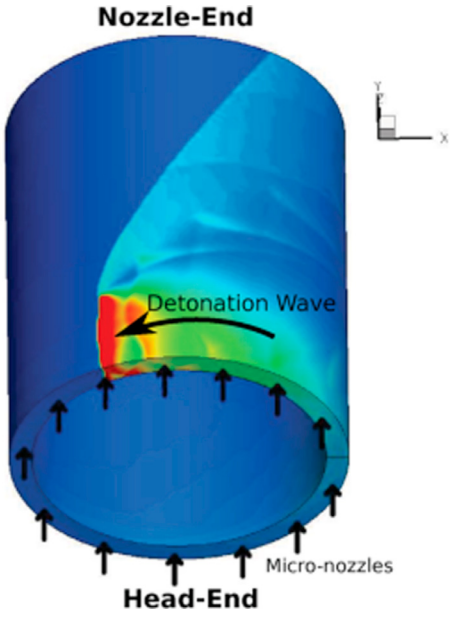

Fig. 1. Example schematic of a rotating detonation engine. The combustion chamber is an annular ring, where the mean direction of flow is from the head end (bottom in figure) to the exit (top). Source: Kailasanath.

flow. Another similar approach for describing the dynamics of weakly nonlinear waves for compressible inviscous flows rotating in an annular ring has been developed in [8] for stratified and in [9] for homogeneous fluids.

In this paper, we will describe the flow paths of particles for continuously rotating flow on a surface of a cylinder that can be used as a descriptor of a detonation engine. The analysis is based on a weakly nonlinear approximated gas dynamic equations with incorporated approximation of Korobeinikov's chemical reaction model that are used to describe the two-dimensional detonation field on a surface of a two-dimensional cylindrical chamber without thickness.

The basis of approximate modeling is to distinguish certain trends that can be described in an analytical form. From the point of view of original equations of motion, such trends are related to exact solutions whereas approximate solutions act as their simplified asymptotic description. The general scheme of such approach is based on the introduction of a small parameter ε in the equations and their solution such that the trend is independent on that parameter and only the orders of smallness terms of the equation for $\varepsilon \to 0$ are being kept into account. If the equations contain terms of different degrees in ε, then only those terms are left, that have the lowest small parameter ε. This gives the desired approximate equations [5,10,11].

2. Model

From the standpoint of a mathematical modeling, the gas motion in the domain $\Omega \subset R^4(x, t)$ is the set of functions $\vec{u}$, ρ, p, ϵ, defined in Ω and satisfying the standard gas dynamic equations with an additional chemical source term $\dot{\omega}$ (see e.g. [10,11]),

$$D\rho + \rho \operatorname{div}(\vec{u}) = \dot{\omega}, \tag{1}$$

$$D\vec{u} + \frac{1}{\rho}\nabla p = 0, \tag{2}$$

$$D\epsilon + \frac{p}{\rho}\operatorname{div}(\vec{u}) = 0, \tag{3}$$

where $\vec{u} = (u^*, v^*, w^*)$ is a velocity vector, ρ is a density, p is a pressure, ϵ is a specific internal energy and

$$D = \frac{\partial}{\partial t} + \vec{u} \cdot \nabla = \frac{\partial}{\partial t} + u^*\frac{\partial}{\partial x} + v^*\frac{\partial}{\partial y} + w^*\frac{\partial}{\partial z}, \tag{4}$$

is the differential operator and $\dot{\omega}$ is the rate of change of a mixture density due to the chemical reaction. We also note that the system (1)–(3) is being closed by the equation of state:

$$p = f(\rho, S), \tag{5}$$

where S is the entropy.

Due to Eq. (1), we can rewrite (3) as

$$D\epsilon + pDV + \frac{p\dot{\omega}}{\rho^2} = 0, \tag{6}$$

where we denote $V = 1/\rho$, so that we associate V with the specific gas volume (the volume of a unit mass). Thus, Eq. (6) represents the balance between the increase in the inertial energy plus the work of expansion of the portion of the gas and the rate of change of the density in gas due to chemical reaction. Next, let us denote the absolute temperature by T. Due to Eq. (5), the first law of thermodynamics yields

$$DS = -\frac{p\dot{\omega}}{T\rho^2}, \tag{7}$$

where T is the absolute temperature.

For further analysis, it is convenient to eliminate the entropy by using the equation: $Dp = f_\rho D\rho + f_s DS$, where the low indexes represent partial derivatives. As follows from the definition of the speed of sound c (see e.g. [10]),

$$c^2 = \left.\frac{dp}{d\rho}\right|_{S=\text{const}} = f_\rho(\rho, S), \tag{8}$$

one can see that the Eq. (7) is equivalent to the relation:

$$Dp = c^2 D\rho - \frac{f_S\, p\dot{\omega}}{T\rho^2}. \tag{9}$$

Thus, we can rewrite the original model (1)–(3) as

$$D\vec{u} + \frac{1}{\rho}\nabla p = 0, \tag{10}$$

$$bDp + \operatorname{div}(\vec{u}) = \left(1 - \frac{f_S\, p}{Tc^2\rho^2}\right)\frac{\dot{\omega}}{\rho}, \tag{11}$$

$$DS = -\frac{p}{T\rho}\frac{\dot{\omega}}{\rho}, \tag{12}$$

in which the values ρ and $b = 1/\rho c^2$ are considered as functions of p and S. We also remark that, the entropy S and the energy $\epsilon = \Xi(V, T)$ are related by the relation (see also [10]),

$$S = R\ln V + \int \Xi'(T) d\ln T, \tag{13}$$

i.e. in reality, the energy depends on the temperature and the solution S of the model (10)–(12) yields also the solution for the energy.

We next use the analogue of the Korobeinikov et al.'s [12] chemical reaction to approximate the chemical source term $\dot{\omega}$ by the relation (see also [13]),

$$\dot{\omega} \approx -\alpha p^{n_1}\rho^{l_1}\exp\left(-\frac{E^*}{RT}\right), \tag{14}$$

in which R is a gas constant, and the parameters α, m_1, n_1, l_1 and E^* (representing the energy activation) are determined from the experimental data [3,14]. Without loss of generality we can normalize the set of the data by taking $n_1 = 1$ and for the sake of simplicity of calculations, we shall set $l_1 = 1$. Usually (see e.g. [12,15]), the relation (13) is used to model equation an accumulation of active radicals in a particle during a chemical reaction. At the initial time, $\omega = 0$, and the induction period stops at $\omega = 1$. After this, the second stage of the reaction begins, which is described by the equation, similar to the relation (13). However, we limit ourselves by a simplified version of the chemical reaction and do not include the higher stages of reactions.

The original model (10)–(12) consists of four nonlinear equations for the unknowns (u, v, p, S), in which $\vec{u} = (u, v)$ is the velocity vector, p is a pressure, ρ is density, S is the entropy, $r = \text{const}$ is a fixed radius of the cylinder, along which we study the gas propagation, and $b = 1/\rho^2 c$ (in which we can consider the sound speed c either to be a constant, or, for example as a function of (p, S) via relation $c^2 = dp/d\rho$).

Another simplifying assumption in this paper is based on considering a special case when the absolute temperature T is sufficiently high, which corresponds to the ignition process in a turbine (e.g. in the moment when an airplane takes off, the absolute temperature is much larger than the numerical values of the pressure and density). In this case, assuming $\alpha > 0$ in (14), the term:

$$F = \frac{1}{T}\exp\left(-\frac{E^*}{RT}\right), \tag{15}$$

appearing in the right side of Eq. (12) can be neglected at certain order of accuracy, by considering the values of T greater than some given value T_ε, for which F is less than some given small value ε, as shown schematically in Fig. 2, which is used to visualize a qualitative behavior of F at different values of parameters E^* and R.

As been discussed in [16], when modeling equilibrium rocket motor performance calculations, usually, viscous forces are taken to be small compared to pressure forces and the heat transferred through the walls is considered to be small compared to the stagnation enthalpy of the gases in the chamber; thus, it is usually assumed that the camber walls are frictionless and

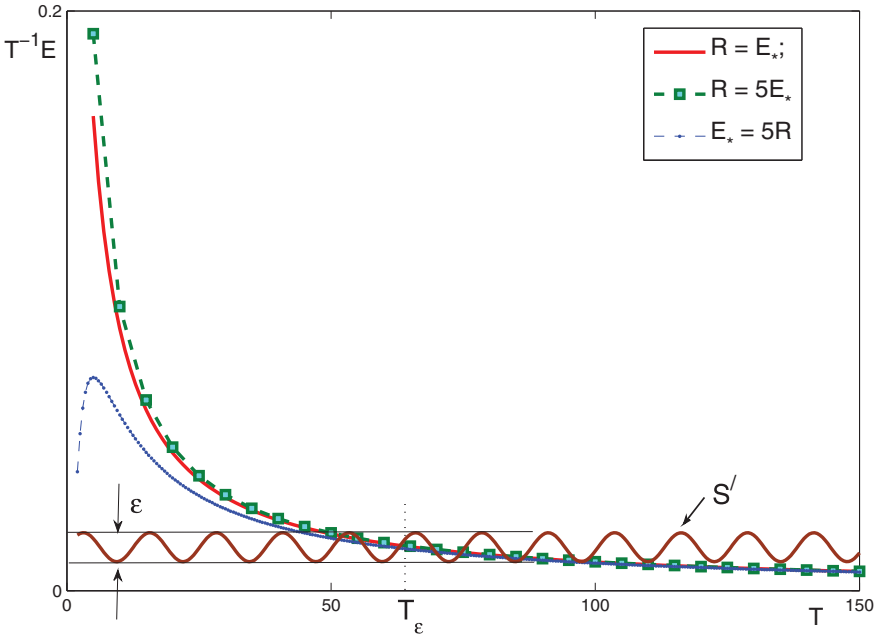

Fig. 2. Qualitative behavior of $F(T)$ at different values of E^* and R.

adiabatic. As a result, as discussed in [14], the gas flow is isentropic and f is weakly dependent on the entropy . Based on this observation, we will simplify the model by assuming that:

$$S = S_0 + \varepsilon S', \tag{16}$$

where $S_0 \approx$ const, ε is a given sufficiently small number (which depends on the experimental data for E^* and R) and S' is a bounded function of the absolute temperature T as demonstrated in Fig. 2. In particular, the recent experimental studies on rotating detonation of rocket performance reported in [17] confirms the validity of the assumption of homogeneous mixing and adiabatic (or almost adiabatic) combustion, i.e. a heat transfer outside of the system is negligible, which corresponds to the case, when $S' \approx$ const in (16).

Thus, up to certain order of accuracy, the last Eq. (12) in the model can be neglected by dropping the right side and assuming $S = S_0$ at the leading order.

Next, in order to describe the gas-filled in an annular chamber without thickness, as shown in Fig. 1, we introduce cylindrical coordinates $x = r\cos\theta$, $y = r\sin\theta$, $z = z$ so that the rate-of-strain tensor is:

$$e_{rr} = \frac{\partial u_r}{\partial r}, \quad e_{\theta\theta} = \frac{1}{r}\frac{\partial u_\theta}{\partial \theta}, \quad e_{r\theta} = \frac{r}{2}\frac{\partial}{\partial r}\left(\frac{u_\theta}{r}\right) + \frac{1}{2r}\frac{\partial u_r}{\partial \theta}. \tag{17}$$

Thus, the resulting approximated two-dimensional version of the model (10)–(12) is written as follows:

$$\rho\left(\frac{\partial u}{\partial t} + \frac{u}{r}\frac{\partial u}{\partial \theta} + v\frac{\partial u}{\partial z}\right) + \frac{1}{r}\frac{\partial p}{\partial \theta} = 0, \tag{18}$$

$$\rho\left(\frac{\partial v}{\partial t} + \frac{u}{r}\frac{\partial v}{\partial \theta} + v\frac{\partial v}{\partial z}\right) + \frac{\partial p}{\partial z} = 0, \tag{19}$$

$$b\left(\frac{\partial p}{\partial t} + \frac{u}{r}\frac{\partial p}{\partial \theta} + v\frac{\partial p}{\partial z}\right) + \frac{1}{r}\frac{\partial u}{\partial \theta} + \frac{\partial v}{\partial z} + p\alpha E = 0, \tag{20}$$

$$\frac{\partial S_0}{\partial t} + \frac{u}{r}\frac{\partial S_0}{\partial \theta} + v\frac{\partial S_0}{\partial z} = 0, \tag{21}$$

where we denote $u = u_\theta$, $v = u_z$, and $E = e^{-\frac{E^*}{RT}}$.

We have to solve this system for the unknowns (u, v, p, S_0), in which $\vec{u} = (u, v)$ is the velocity vector, p is a pressure, ρ is density, S_0 is the entropy, $r =$ const is a fixed radius of the cylinder, along which we study the gas propagation, and $b = 1/\rho^2 c$ (in which we can consider the sound speed c either to be a constant, or, for example as a function of (p, S) via relation $c^2 = dp/d\rho$).

The parameters $n_1 = 1, \alpha, E^*, R$ and T are constants, in which R is a gas constant and T is an absolute temperature.

3. Weakly nonlinear model

In this section, we apply the formal method of approximate modeling of the gas flow with the incorporated Korobeinikov's chemical reaction model in an annular chamber without thickness, as described by nonlinear Eqs. (18)–(21). It is convenient to rewrite the model (18)–(21) in a matrix notation

$$\frac{\partial \vec{U}}{\partial t} + A^{\theta}\frac{\partial \vec{U}}{\partial \theta} + A^{z}\frac{\partial \vec{U}}{\partial z} + B\vec{U} = 0, \tag{22}$$

for the unknown vector $\vec{U} = (u, v, p, S_0)$, where

$$A^{\theta} = \begin{pmatrix} \frac{u_\theta}{r} & 0 & \frac{1}{\rho r} & 0 \\ 0 & \frac{u_\theta}{r} & 0 & 0 \\ \frac{1}{br} & 0 & \frac{u_\theta}{r} & 0 \\ 0 & 0 & 0 & \frac{u_\theta}{r} \end{pmatrix}, \quad A^{z} = \begin{pmatrix} u_z & 0 & 0 & 0 \\ 0 & u_z & \frac{1}{\rho} & 0 \\ 0 & \frac{1}{b} & u_z & 0 \\ 0 & 0 & 0 & u_z \end{pmatrix}, \quad B = \begin{pmatrix} 0 & 0 & 0 & 0 \\ 0 & 0 & 0 & 0 \\ 0 & 0 & \frac{\alpha}{b}E & 0 \\ 0 & 0 & 0 & 0 \end{pmatrix}, \tag{23}$$

where subscripts denote partial derivatives.

We start with the assumption that some basic flow (i.e. exact solution of the model (22)) is given:

$$\vec{u} = \vec{u}_0(\theta, z, t), \quad p = p_0(\theta, z, t), \quad \rho = \rho_0(\theta, z, t), \quad S = S_0^*(\theta, z, t). \tag{24}$$

We look for another solution that is close to (24) in the form (see e.g. [18,19]),

$$\vec{u} = \vec{u}_0 + \varepsilon\vec{u}', \quad p = p_0 + \varepsilon p', \quad \rho = \rho_0 + \varepsilon\rho', \quad S = S_0^* + \varepsilon S_0', \tag{25}$$

in which the prime is used for new unknown functions and ε is a small parameter. As discussed in Section 1, this procedure is largely formal. Mathematics ideal requires proof that the solution of the complete equations in question for $\varepsilon \to 0$ has a solution of the approximate equations at zeroth order of ε (at least asymptotically). In fact, this ideal is achieved in very rare cases; researchers usually limited to the formal construction of an approximate model (however, some instances, such as [20] exist, where a full proof of such a convergence is given). It is clear that, at the same time, the role of the criterion of practice is greatly increased.

Example 1. As an example, we find some particular class of exact solution of the model (22). Let us consider the case, when

$$\rho_0 = \text{cont}, \; c_0 = \text{cont}, \; S_0^* = \text{const}. \tag{26}$$

As been discussed in [16], when modeling equilibrium rocket motor performance calculations, usually, viscous forces are taken to be small compared to pressure forces and the heat transferred through the walls is considered to be small compared to the stagnation enthalpy of the gases in the chamber; thus, it is usually assumed that the camber walls are frictionless and adiabatic. As a result, as discussed in [14], the gas flow is isentropic. We next assume the rest of the solution in the form:

$$v_0 = \text{cont}, \; u_0 = U(t), \; p_0 = P(\theta, t). \tag{27}$$

Substituting the presentations (26) and (27) in (22) (or, alternatively, in (18)–(21)), we obtain

$$u_0 = \frac{c_1}{\rho_0\beta}e^{-\beta t}, \quad p_0 = c_1 e^{-\beta t}\left(\theta - \frac{c_1}{\rho_0 r\beta^2}e^{-\beta t}\right), \tag{28}$$

where c_1 is an arbitrary constant and

$$\beta = \frac{\alpha}{b_0}e^{-\frac{E^*}{RT}}. \tag{29}$$

So, the functions (26) and (28) constitute the particular class of exact solution of the nonlinear model (22).

Hereafter, we also assume that:

$$c = c_0 + \varepsilon^k c', \tag{30}$$

in which $k = 1, 2$.

In this paper, we consider the particular case when $k = 2$. Particularly, as been discussed in [16], when modeling RDEs, it can be assumed that the spray is dilute enough that droplet interactions may be ignored, that the gases follow the perfect gas law so that the speed of sound c can be approximated by the constant value c_0. In more general case, when $k = 1$, the value $1/b$ can be approximated as ([11,18]):

$$\frac{1}{b} \approx \frac{1}{b_0} - \frac{\varepsilon}{b_0}\left(\frac{\rho'}{\rho_0} + 2\frac{c'}{c_0}\right), \tag{31}$$

so that that simplifying assumption $k = 2$ corresponds to the case when $c' << c_0$ in (31).

We substitute the presentation (25)–(30) into Eq. (22) and remark, that under a such substituting, the operator

$$D = \frac{\partial}{\partial t} + \vec{u}\cdot\nabla = \frac{\partial}{\partial t} + \frac{u}{r}\frac{\partial}{\partial \theta} + v\frac{\partial}{\partial z}, \tag{32}$$

becomes

$$D = D_0 + \varepsilon\,\vec{u}\,'\cdot\nabla, \quad D_0 = \frac{\partial}{\partial t} + \frac{u^0}{r}\frac{\partial}{\partial \theta} + v^0\frac{\partial}{\partial z}, \tag{33}$$

and the function (25) is a solution of the model (22). Thus, we arrive to the following equations for small perturbations:

$$D_0\,\vec{u}\,' + \vec{u}\,'\cdot\nabla\vec{u}_0 + \frac{1}{\rho_0}\nabla p' - \frac{\rho'}{\rho_0^2}\nabla p_0 = 0, \tag{34}$$

$$D_0 p' + \frac{1}{b_0}\operatorname{div}\vec{u}\,' + \vec{u}\,'\cdot\nabla p_0 + \left(\frac{k}{b_0}p' - \frac{\alpha p_0\rho'}{b_0\rho_0}\right)E = 0, \tag{35}$$

$$D_0 S_0' + \vec{u}\,'\cdot\nabla S_0^* = 0, \tag{36}$$

where $b_0 = c_0^2\rho_0$. Also, the pressure perturbation p is related with perturbations for ρ and S by the equation of state (5), which is:

$$p' = \frac{1}{\varepsilon}\left[f\left(\rho_0 + \varepsilon\rho',\ S_0^* + \varepsilon S_0'\right) - f\left(\rho_0 + \varepsilon\rho',\ S_0^* + \varepsilon S_0'\right)\right]. \tag{37}$$

We can exclude the density perturbation ρ' from the model (34)–(36) by means of the equation:

$$p' = c_0^2\rho' + f_{S_0^*}S_0', \tag{38}$$

in which $f_{S_0^*} = f_{S_0}\left(\rho_0, S_0^*\right)$ and the subscript means partial derivative.

Then, in virtue of (38), the system (34)–(36) for the unknown vector $\vec{U}\,' = \left(u', v', p', S_0'\right)$ is written in a matrix notation as:

$$\frac{\partial\vec{U}\,'}{\partial t} + A_0^\theta\frac{\partial\vec{U}\,'}{\partial\theta} + A_0^z\frac{\partial\vec{U}\,'}{\partial z} + B_0\vec{U}\,' = 0, \tag{39}$$

where

$$A_0^\theta = \begin{pmatrix} \frac{u_0}{r} & 0 & \frac{1}{r\rho_0} & 0 \\ 0 & \frac{u_0}{r} & 0 & 0 \\ \frac{1}{rb_0} & 0 & \frac{u_0}{r} & 0 \\ 0 & 0 & 0 & \frac{u_0}{r} \end{pmatrix}, \quad A_0^z = \begin{pmatrix} v_0 & 0 & 0 & 0 \\ 0 & v_0 & \frac{1}{\rho_0} & 0 \\ 0 & \frac{1}{b_0} & v_0 & 0 \\ 0 & 0 & 0 & v_0 \end{pmatrix}, \tag{40}$$

$$B_0 = \begin{pmatrix} \frac{1}{r}\frac{\partial u_0}{\partial\theta} & \frac{\partial u_0}{\partial z} & -\frac{1}{r\rho_0 b_0}\frac{\partial p_0}{\partial\theta} & \frac{f_{S_0^*}}{r\rho_0 b_0}\frac{\partial p_0}{\partial\theta} \\ \frac{1}{r}\frac{\partial v_0}{\partial\theta} & \frac{\partial v_0}{\partial z} & -\frac{1}{\rho_{0b_0}}\frac{\partial p_0}{\partial z} & \frac{f_{S_0^*}}{\rho_0 b_0}\frac{\partial p_0}{\partial z} \\ \frac{1}{r}\frac{\partial p_0}{\partial\theta} & \frac{\partial p_0}{\partial z} & \frac{\alpha}{b_0}\left(1 - \frac{p_0}{b_0}\right)E & \frac{\alpha f_{S_0^*}}{b_0^2}p_0 E \\ \frac{1}{r}\frac{\partial S_0^*}{\partial\theta} & \frac{\partial S_0^*}{\partial z} & 0 & 0 \end{pmatrix}. \tag{41}$$

Example 2. Let us consider the particular case when

$$\vec{u}_0 = 0,\ p_0 = \text{const},\ S_0^* = \text{const}. \tag{42}$$

In this case, $D = \partial/\partial t$. Let us look for isentropic perturbations, i.e. when $S' = 0$. In this case, the system (34)–(36) is equivalent to the acoustic equations and can easily be reduced to a single equation for the pressure perturbation only

$$\frac{\partial^2 p'}{\partial t^2} = \frac{1}{b_0\rho_0}\Delta p' - \frac{\alpha}{b_0}\left(1 - \frac{p_0}{b_0}\right)E\frac{\partial p'}{\partial t}, \tag{43}$$

where

$$\Delta = \left(\frac{1}{r^2}\frac{\partial^2}{\partial\theta^2} + \frac{\partial^2}{\partial z^2}\right),$$

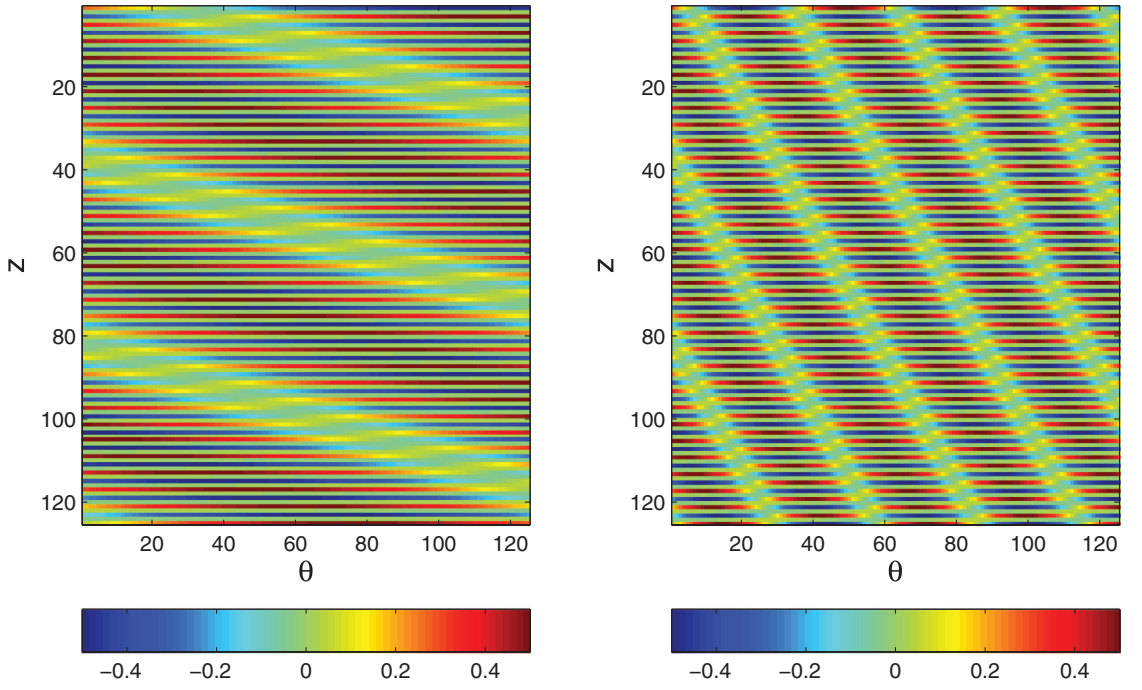

Fig. 3. Contour plot of the pressure perturbation p' in (θ, z) plane at the values $d_2 = 0.2$ (left panel) and $d_2 = 1.1$ (right panel). (For interpretation of the references to color in this figure legend, the reader is referred to the web version of this article.)

is the Laplace operator. We also remark that Eq. (43) with $\alpha = 0$ (or when $p_0 \sim b_0$) represents the classic equation for internal waves with zero Coriolis effects [11,18].

One particular class of solution of Eq. (43) can easily be obtained if we look for some specific forms of p'. For example, let us look for solution in the form:

$$p'(\theta, z, t) = A(t)e^{i\varphi(\theta,z)}, \tag{44}$$

where the phase φ and the amplitude A are real (see e.g. p. 519 in [21]). No generality is lost by assuming A to be real. Indeed, following [21], suppose it is complex and of the form $A = \widetilde{A}\exp(i\mu)$ where $\widetilde{A}$ and μ are real. Then $p' = \widetilde{A}\exp\left[i(\varphi + \mu)\right]$, a form in which $(\varphi + \mu)$ is the phase. Substituting into (43) and equating the real and imaginary parts, we get:

$$\frac{d^2A}{dt^2} + \frac{\alpha}{b_0}\left(1 - \frac{p_0}{b_0}\right)E\frac{dA}{dt} + \frac{A}{b_0\rho_0}\left[\frac{1}{r^2}\left(\frac{\partial\varphi}{\partial\theta}\right)^2 + \left(\frac{\partial\varphi}{\partial z}\right)^2\right] = 0, \tag{45}$$

$$\frac{1}{r^2}\frac{\partial^2\varphi}{\partial\theta^2} + \frac{\partial^2\varphi}{\partial z^2} = 0. \tag{46}$$

One particular solution of the Laplace equation (46) is

$$\varphi = d_1 r\theta + d_2 z + d_3, \tag{47}$$

where $d_i = \text{const.}(i = 1, 2, 3)$. Since the solution φ is known, the Eq. (45) can readily be solved and so, in terms of d_i, the particular solution for p' can be written as:

$$p' = d_4 e^{\frac{t}{2}\left[\frac{\alpha}{b_0}\left(\frac{p_0}{b_0}-1\right)E + \left(\frac{\alpha^2}{b_0^2}\left(\frac{p_0}{b_0}-1\right)^2E^2 - 4\frac{d_1^2+d_2^2}{b_0\rho_0}\right)^{\frac{1}{2}}\right]}\cos\left(d_1 r\theta + d_2 z + d_3\right), \tag{48}$$

where $d_4 = \text{const.}$ The constants $d_j = \text{const.}(i = 1, 2, 3, 4)$ can be determined from the boundary and initial conditions.

The next plot shown in Fig. 3 is used to illustrate the effects of parameters on the qualitative behavior of the pressure perturbation p' at $t = 0.5$ s. The light green beams on the plot correspond to the points on the medium that exhibit the maximum amount of negative or downward displacement from the rest position. In particular, we remark that the slopes, width and the number of the beams change dramatically depending on the parameters of the model, for example, parameter d_2, as illustrated in this plot. Exact pressure profiles are not common in weakly nonlinear models, but they have been discussed in [22,23].

Since our modeling is not related to the direct description of the thermodynamic performance of rotating detonation engines, but we are rather interested in analytic treatment of the governing equations, we do not incorporate here specific boundary

conditions and thus we leave the constants of integrations to be arbitrary. The parameters of the model are also chosen to be arbitrary. In particular, we use the following values of parameters for visualizing the solution p' given by (48): $T = 20^{\circ}$C, $c_0 = 343$ m/s, $\rho_0 = 1.2$ kg/m^3, $R = 8.3$ m$^3 \cdot$ Pa $\cdot$ mol$^{-1} \cdot$ K^{-1}, $r = 3$ m, $\alpha = 5$, $d_2 = 0.2$, $d_3 = 1$, $d_4 = 0.5$, $E = 2.0$, and the values of constants d_2 are taken to be 0.2 (left panel) and $d_2 = 1.1$ (right panel), as shown in Fig. 3. However, careful analysis of boundary conditions for similar modeling of the flow in cylindrical domain for stratified fluids affected by the Coriolis forces and analysis of longitudinal atmospheric waves circulating around a solid circle large radius (so that the gravity is directed to the center of the circle) under different physical and meteorological situations were done in our previous studies in [5,8,9,24].

4. Bicharacteristics

It is assumed that the shape of the wave front is known (e.g. from the experiment) at initial time $t = 0$. In order to determine the wave front at any time $t > 0$, we construct the bicharacteristics (in a wave theory, bicharacteristics are also known as beams along which small perturbations propagate in the media) of the weakly nonlinear model (39). To this end, we form the characteristic equation:

$$\det\left(\xi A_0^{\theta} + \eta A_0^{z} + \tau I\right) = 0, \tag{49}$$

where $\overrightarrow{\nu} = (\xi, \eta, \tau)$ is the vector aligned along the characteristic direction corresponding to the system (39), provided that the relation (49) is satisfied. This means that the surface S: $\psi(\theta, z, t) \in \mathbb{R}^3$ is the characteristic surface for the system (39) if at each of its point, the normal vector $\overrightarrow{\nu}$ satisfies the characteristic equation:

$$\tau = \chi(\xi, \eta), \tag{50}$$

where χ is the homogeneous function of the first order (see also [25]) and the following relations hold:

$$\tau = \frac{\partial \psi}{\partial t}, \quad \xi = \frac{\partial \psi}{\partial \theta}, \quad \eta = \frac{\partial \psi}{\partial z}. \tag{51}$$

As been pointed earlier, the position and the shape of the front is given by:

$$\psi(\theta, z, t) = 0, \tag{52}$$

and is known at $t = 0$. Solving Eq. (49), we determine four roots χ of the characteristic Eq. (49) as follows:

$$\tau_1 = \tau_2 = -\frac{\xi u_0 + \eta v_0 r}{r}, \tag{53}$$

$$\tau_{3,4} = -\frac{b_0\rho_0(\eta v_0 r + \xi u_0) \pm \sqrt{b_0\rho_0(\eta^2 r^2 + \xi^2)}}{b_0\rho_0 r}.$$

In order to derive the general form for the expressions along the (θ, z) particle path, we recall (see e.g. [10,11,25]) that *equations of beams* (direction of propagation for small perturbations of the system in the media) for the hyperbolic system:

$$\partial_t u + \sum_{\alpha=1}^{3} A^{\alpha}\partial_{\alpha} u + Bu = 0, \tag{54}$$

has the form:

$$\frac{dt}{ds} = 1, \quad \frac{dx_i}{ds} = -\frac{\partial \chi}{\partial \psi_i}, \quad \frac{d\psi_{\alpha}}{ds} = \frac{\partial \chi}{\partial x_{\alpha}}, \quad \frac{d\psi_t}{ds} = \chi_t, \quad \frac{d\psi}{ds} = 0, \tag{55}$$

where we have used Ovsyannikov's notation [10]. In particular, $\partial_t = \frac{\partial}{\partial t}$ and $\partial_{\alpha} = \frac{\partial}{\partial x_{\alpha}}$, so that the form:

$$\frac{\partial \psi}{\partial t} = \chi\left(\frac{\partial \psi}{\partial x_1}, \frac{\partial \psi}{\partial x_2}, \frac{\partial \psi}{\partial x_2}\right), \tag{56}$$

in [10] is used to denote the characteristic equation of the hyperbolic system (54), in which the right side of (56) represents the normal vector to the hyperplane $\psi\left(\overrightarrow{x}, t\right) = 0$, as in (52).

So, the idea was to reduce the equations for small perturbations of the original model (18)–(21) to the form (54). In particular, in Eqs. (54) and (55) the following notation is used:

$$\overrightarrow{x} = (x_1, x_2, x_3) \in \mathbb{R}^3, \ u\left(\overrightarrow{x}, t\right) \in \mathbb{R}^n, \ \partial_t = \frac{\partial}{\partial t}, \quad \partial_{\alpha} = \frac{\partial}{\partial x_{\alpha}}, \quad \alpha = 1, 2, 3 \tag{57}$$

and A and B are $n$dimensional matrices that depends on $\overrightarrow{x}$ and t and s in (57) is a parameter along the curve.

In particular, for the first root of multiplicity two $\tau_1 = \tau_2$, integration of the second equation of the system (55) yields the equations of bicharacteristics for the trajectory along θ and z in the form:

$$\theta - \theta_0 = \frac{1}{r}\int_0^t u_0\left(\theta, z, t'\right)dt', \quad z - z_0 = \int_0^t v_0\left(\theta, z, t'\right)dt', \tag{58}$$

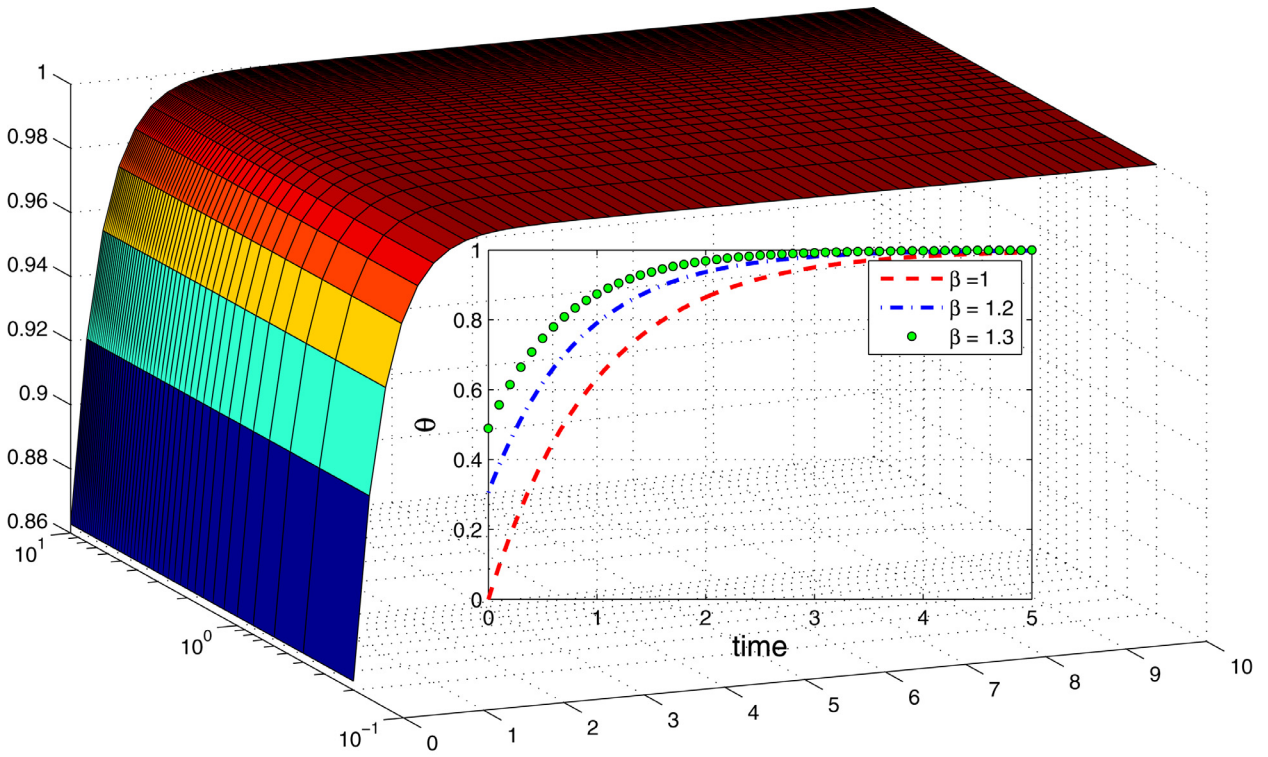

Fig. 4. The dynamics of the wave front associated with the exact solution in Example 1. In this case, $z = 0$ and the resulting front moves azimuthally along the cylindric surface.

where we drop the constants of integration.

Similarly, for the third and fourth roots $\tau_{3,4}$, we obtain,

$$\theta - \theta_0 = -\left[\int_0^t \frac{u_0}{r}dt' \pm \frac{1}{r\sqrt{b_0\rho_0}}\int_0^{t'} \frac{\xi}{\sqrt{\xi^2 + r^2\eta^2}}dt'\right], \tag{59}$$

$$z - z_0 = -\left[\int_0^t v_0 dt' \pm \frac{1}{\sqrt{b_0\rho_0}}\int_0^{t'} \frac{r\eta}{\sqrt{\xi^2 + r^2\eta^2}}dt'\right], \tag{60}$$

which means that, for the roots $\tau_{3,4}$, the trajectories are parallel to the gradient vector.

We remark, that the formulae (59) and (60) for the trajectories are somewhat similar to formulae for particle trajectories discussed in [26,27].

For visualization purposes, we plot the wave fronts for the simple case, corresponding to the first root $\tau_1 = \tau_2$, given by (58) for the particular velocity field u_0 and v_0 provided in Example 1 by formulae (27) and (28), respectively. For this particular solution, the Eq. (59) can be reduced to the form:

$$f(\theta; r, t, \rho_0, \beta) = 0, \tag{61}$$

in which

$$f(\theta; r, t, \rho_0, \beta) = \theta + \frac{e^{-\beta t}}{r^2\rho_0^2\beta^2} - 1, \quad \theta_0 = 0 \tag{62}$$

whereas the second Eq. (60) yields $z = \text{const}$, which, without loss of generality, we can set to be zero. The plot in Fig. 4 is used to illustrate the qualitative azimuthal dynamics of the wave front associated with the function f given by (62). Again, since we are only interested in a qualitative analysis, for the better visualization purposes, we choose arbitrarily the following numeric values of parameters: $r = 1$, $\rho_0 = 1$ and $\beta = 2.7$. The internal plot in in Fig. 4 shows the effect of parameter β on the spinning dynamics along θ.

The plot in Fig. 5 shows the level curves $f(\theta; r, t, \rho_0, \beta) = 0$ in polar coordinates at different values of parameters. For example, the subplot (a) shows the curves at the values of parameters $r = 1$, $\rho_0 = 1$, $\beta = 1$ and $t = 0$, 1 and 10, subplot (b) shows the curves at the values of parameters $t = 1$, $\rho_0 = 1$, $\beta = 1$ and $r = 1$ and 10, and so on.

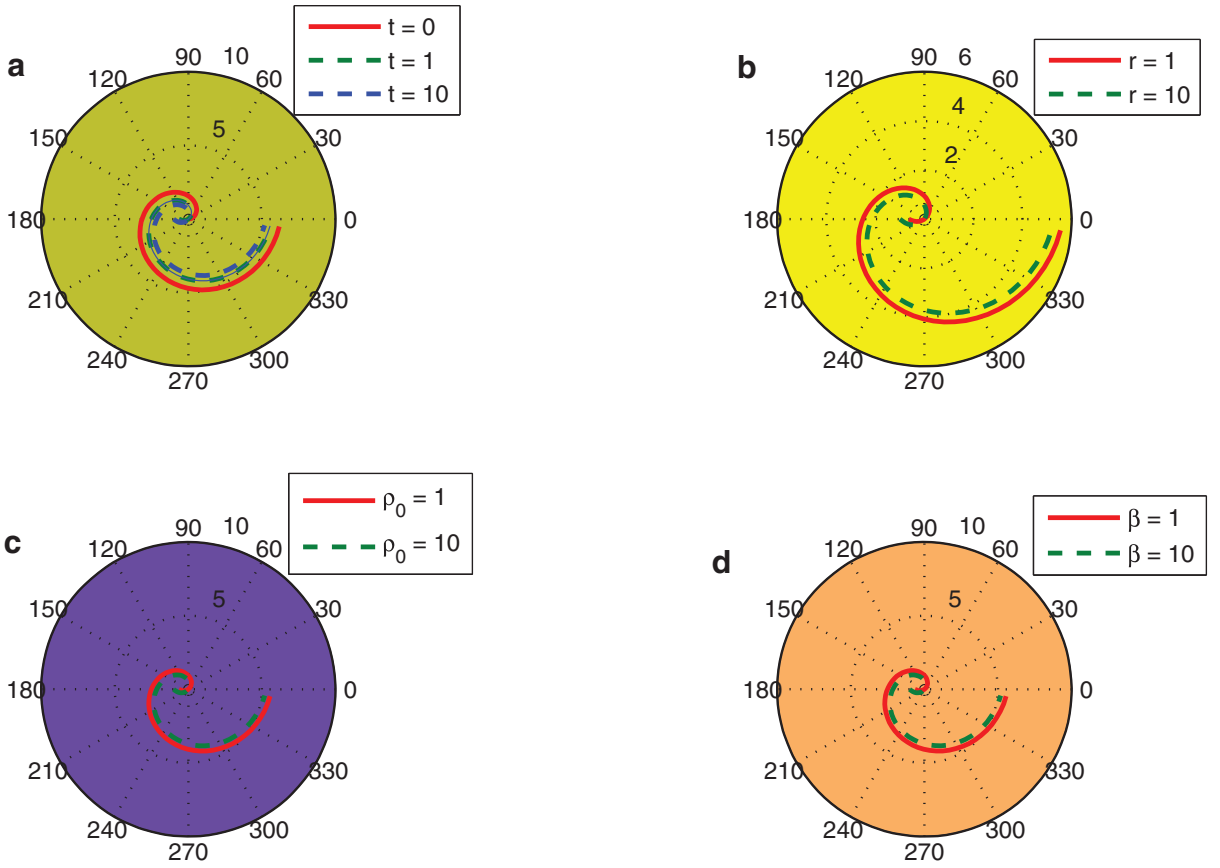

Fig. 5. Illustration of the trajectory.

Thus, in some particular cases, the wave fronts (bicharacteristics) can be found in explicit form. However, in general cases, the problem is reduced to finding the solution (for example, using asymptotic methods or numeric approach) and the determination of the wave front $\psi(\theta, z, 0) = 0$ at initial time (for example, using experimental data).

5. Discussions

We have developed an analytic approach for investigating the wave front propagation that can be used for understanding an overall description of the flow-field within a continuously rotating detonation. Our model consists of the standard gas dynamic equations with an additional chemical source term $\dot{\omega}$, which we described by an approximation of the Korobeinikov's chemical reaction model that is usually used in two-dimensional detonation field on a surface of a two-dimensional cylindrical chamber without thickness ([12]). In the frame of the present modeling of RDEs, the method of wave front propagation proposed in this paper is well understood in the shallow water theory. For the model studied here, the latter method allows to reduce the original nonlinear model to weakly nonlinear four-dimensional wave equation that can be solved nearly exactly.

In real-world situations, the complicated flow-field of continuously rotating detonations engines consists not only of a detonation wave, a deflagration wave, and oblique shock wave, but also of characteristic surfaces that are usually classified as (i) sound characteristics, (ii) contact characteristics and (iii) thermal compression wave, spreading in a given gas flow [3,28] . However, the paths of flow particles (that are along the beams) for rotating detonation have not been studied previously [4,6]. We found that the beam can be expressed analytically in explicit form for special classes of flow (e.g. isentropic gas flow) and special form of exact solutions of the gas dynamics model in question. However, in more general cases, the dynamics of wave fronts can still be determined provided that the wave front is known at initial time and the solution is known somehow (either from experimental and numeric analysis). One of our particular interests for further development of this approach, is to apply the Lie group analysis and find wider classes of exact solutions of the model (18)–(21). A similar approach was applied to the nonlinear Navier–Stokes equations with applications to general circulation model on a surface of rotating sphere [25] and to the modeling of nonlinear stratified fluid flows confined in a cylindric volume of fluid [5]. Additionally, some exact solutions were deduced in [29] by means of the Lie group analysis for the modeling of thermal explosion with reactant consumption. So this approach seems to be feasible.

As a preliminary result on application of the Lie group analysis, we consider here the original nonlinear model (18)–(21) within some approximations.

The basic ones are:

$$c = c_0, \tag{63}$$

and

$$p = f(\rho). \tag{64}$$

Within the approximation (16),(63) and (64) with where $S_0 = \text{const}$, the resulting two-dimensional nonlinear model (18)–(21) is written as:

$$\rho\left(\frac{\partial u}{\partial t} + \frac{u}{r}\frac{\partial u}{\partial \theta} + v\frac{\partial u}{\partial z}\right) + \frac{1}{r}\frac{\partial}{\partial \theta}f(\rho) = 0, \tag{65}$$

$$\rho\left(\frac{\partial v}{\partial t} + \frac{u}{r}\frac{\partial v}{\partial \theta} + v\frac{\partial v}{\partial z}\right) + \frac{\partial}{\partial z}f(\rho) = 0, \tag{66}$$

$$\frac{1}{\rho^2 c_0}\left(\frac{\partial f(\rho)}{\partial t} + \frac{u}{r}\frac{\partial f(\rho)}{\partial \theta} + v\frac{\partial f(\rho)}{\partial z}\right) + \frac{1}{r}\frac{\partial u}{\partial \theta} + \frac{\partial v}{\partial z} + \alpha E f(\rho) = 0, \tag{67}$$

The essential result of Lie's group classification is that the model (65)–(67) is nonlinear self-adjoint (see the definition of nonlinear self-adjointness in [30]) only in case of certain $f(\rho)$, namely when

$$f(\rho) = -c_0\rho^2 + c_1,\ c_1 = \text{const}. \tag{68}$$

Without loss of generality, we can set $c_1 = 0$ in (68). Then the model (65)–(67) with

$$f(\rho) = -c_0\rho^2, \tag{69}$$

is written as:

$$r\frac{\partial u}{\partial t} + u\frac{\partial u}{\partial \theta} + ru\frac{\partial u}{\partial z} - 2c_0\frac{\partial \rho}{\partial \theta} = 0, \tag{70}$$

$$r\frac{\partial v}{\partial t} + u\frac{\partial v}{\partial \theta} + rv\frac{\partial v}{\partial z} - 2c_0 r\frac{\partial \rho}{\partial z} = 0, \tag{71}$$

$$2\left(r\frac{\partial \rho}{\partial t} + u\frac{\partial \rho}{\partial \theta} + rv\frac{\partial \rho}{\partial z}\right) + \left(\rho\frac{\partial u}{\partial \theta} + r\rho\frac{\partial v}{\partial z} - \alpha r E c_0\rho^3\right) = 0, \tag{72}$$

where $E \neq 0, \alpha \neq 0, c_0 \neq 0$ and $r \neq 0$.

The invariants are calculated as:

$$\lambda = t^{-3/2}(r^2\theta^2 + z^2), \tag{73}$$

$$J_1 = t^{1/2}\rho, \quad J_2 = t^{1/2}(u^2 + v^2), \quad J_3 = t^{-1/2}(r\theta v - zu). \tag{74}$$

Invariant solution has the form:

$$J_1 = F(\lambda), \quad J_2 = G(\lambda), \quad J_3 = H(\lambda). \tag{75}$$

Hence,

$$\rho = t^{-\frac{1}{2}}F(\lambda), \tag{76}$$

$$u^2 + v^2 = t^{-\frac{1}{2}}G(\lambda), \tag{77}$$

$$r\theta v - zu = t^{\frac{1}{2}}H(\lambda). \tag{78}$$

For any $G(\lambda)$ from (76)–(78) it is possible to find function $Q(\lambda)$ such that:

$$G(\lambda) = \frac{1}{\lambda}\left(Q^2(\lambda) + H^2(\lambda)\right).$$

Then, explicit expressions can be written for u and v as:

$$u = \frac{t^{1/2}}{r^2\theta^2 + z^2}(-zH(\lambda) \pm r\theta Q(\lambda)), \tag{79}$$

$$v = \frac{t^{1/2}}{r^2\theta^2 + z^2}(r\theta H(\lambda) \pm zQ(\lambda)). \tag{80}$$

Substituting (76), (79) and (80) into system (70) and (71) we derive system of ordinary differential equations on functions $F(\lambda)$, $H(\lambda)$, $Q(\lambda)$, also containing variables t, θ, z. Knowing that

$$t = \frac{(r^2\theta^2 + z^2)^{2/3}}{\lambda^{2/3}}, \tag{81}$$

we can eliminate variable t from derived equations and then split with respect to remaining variables θ and z. Thus we derive the following system:

$$(\pm 4Q - 3\lambda)H' + H = 0, \tag{82}$$

$$-8c_0\lambda^2F' + \left(4\lambda Q \mp 3\lambda^2\right)Q' \pm \lambda Q - 2H^2 - 2Q^2 = 0, \tag{83}$$

$$(\mp 4Q + 3\lambda)F' \pm 2FQ' - c_0E\alpha F^3 + F = 0. \tag{84}$$

Case 1. If $H' \neq 0$, then from (82) we have:

$$Q(\lambda) = \pm\frac{1}{4}\left(3\lambda - \frac{H}{H'}\right). \tag{85}$$

Remaining Eqs (83) and (84) take the form:

$$2\lambda H^2H'' + \left(16H^2 + 2\lambda^2 + 64c_0\lambda^2F'\right)H'^3 + H^2H' = 0, \tag{86}$$

$$FHH'' + 2\left(2 - Ec_0\alpha F^2\right)FH'^2 + 2HF'H' = 0. \tag{87}$$

Thus invariant solution of system (70) and (71) has the form:

$$\rho = t^{-\frac{1}{2}}F(\lambda), \tag{88}$$

$$u = \frac{3}{4}\frac{r\theta}{t} - \frac{t^{1/2}}{r^2\theta^2 + z^2}\left(z + \frac{1}{4}\frac{r\theta}{H'(\lambda)}\right)H(\lambda), \tag{89}$$

$$v = \frac{3}{4}\frac{z}{t} + \frac{t^{1/2}}{r\theta}\left[1 - \frac{z}{r^2\theta^2 + z^2}\left(z + \frac{1}{4}\frac{r\theta}{H'(\lambda)}\right)\right]H(\lambda), \tag{90}$$

where

$$\lambda = t^{-3/2}(r^2\theta^2 + z^2), \tag{91}$$

and functions $H(\lambda)$, $F(\lambda)$ satisfy system (86) and (87).

Case 2. If $H' = 0$, then from (82) we derive that $H = 0$ and system (82)–(84) takes the form

$$-8c_0F' + (4Q \mp 3\lambda)\lambda Q' \pm \lambda Q - 2Q^2 = 0, \tag{92}$$

$$(\mp 4Q + 3)F' \pm 2FQ' - c_0E\alpha F^3 + F = 0. \tag{93}$$

Thus invariant solution of system (70) and (71) has the form:

$$\rho = t^{-\frac{1}{2}}F(\lambda), \tag{94}$$

$$u = \pm\frac{r\theta t^{1/2}}{r^2\theta^2 + z^2}Q(\lambda), \tag{95}$$

$$v = \pm\frac{zt^{1/2}}{r^2\theta^2 + z^2}Q(\lambda), \tag{96}$$

where λ is given by (91) and functions $F(\lambda)$ and $Q(\lambda)$ satisfy system (92) and (93).

Another interesting direction for further studies is to incorporate the recent numeric results in [31], where the authors provide the numeric results on flow distribution and initial positions of the just injected fuel with a stable propagating detonation wave. Since the results are given in terms pressure contours and streamlines, this will allow us to make an analytic approximation for the initial wave front $\psi(\theta, z, 0) = 0$ and the initial distribution of the flow field.

Acknowledgment

The author is grateful to Narendra Joshi from GE Corporate for productive discussions on the topic.

References

[1] L. Massa, F.K. Lu, Role of the induction zone on detonation–turbulence linear interaction, Combust. Theory Model. 15 (3) (2011) 347–371.
[2] C.A. Norden, D. Schwer, F. Schauer, B. Hoke, B. Cetegen, T. Barber, Thermodynamic modeling of a rotating detonation engine, in: Proceedings of the 49th AIAA Aerospace Sciences Meeting including the New Horizons Forum and Aerospace Exposition (AIAA 2011-0803), 2011.
[3] D.M. Davidenko, I. Gokalp, A.N. Kudryavtsev, Numerical study of the continuous detonation wave rocket engine, in: Proceedings of 15th AIAA International Space Planes and Hypersonic Systems and Technologies Conference, 2008, p. 268.
[4] K. Kailasanath, E.S. Oran, J.P. Boris, T.R. Young, Determination of detonation cell size and the role of transverse waves in two-dimensional detonations, Combust. Flame 61 (3) (1985) 199–209.
[5] R.N. Ibragimov, G. Jefferson, J. Carminati, Invariant and approximately invariant solutions of non-linear internal gravity waves forming a column of stratified fluid affected by the Earth's rotation, Int. J. Nonlinear Mech. 51 (2013) 28–44.
[6] D. Shcwer, K. Kailasanath, Numerical investigation of rotating detonation engines, in: Proceedings of the 46th AIAA/ASME Joint Propulsion Conference and Exhibit, 2010.
[7] S.A. Zhdan, F.A. Bykovskii, E.F. Vedernikov, Mathematical modeling of a rotation detonation wave in a hydrogen–oxygen mixture, Combust. Explos. Shock Waves 43 (4) (2007) 449.
[8] R.N. Ibragimov, Free boundary effects on stability of two phase planar fluid motion in annulus: migration of the stable mode, Commun. Nonlinear Sci. Numer. Simul. 15 (9) (2010) 2361–2374.
[9] R.N. Ibragimov, L. Guang, Splitting phenomenon of a higher-order shallow water theory associated with a longitudinal planetary waves, Dyn. Atmos. Oceans 69 (2015) 1–11.
[10] L.V. Ovsyannikov, Lectures on the Fundamentals of Gas Dynamics, Nauka, Moscow, 1981. (in Russian).
[11] N.H. Ibragimov, R.N. Ibragimov, Applications of Lie Group Analysis in Geophysical Fluid Dynamics, Series on Complexity, Nonlinearity and Chaos, vol. 2, World Scientific Publishers, 2011.ISBN: 978-981-4340-46-5
[12] V.P. Korobeinikov, V.A. Levin, V.V. Markov, G.G. Chernyi, Propagation of blast waves in a combustible gas, Astronaut. Acta 17 (1972) 529–537.
[13] W.H. Heiser, D.T. Pratt, Thermodynamic cycle analysis of pulse detonation engines, J. Propuls. Power 18 (1) (2002) 68.
[14] R.M. Clayton, Experimental Observations Relating to Inception of Liquid Rocket Engine Popping and Resonant Combustion to the Stagnation Dynamics of Injection Impingement, JPL Technical Report, pp. 32–1479, 1970.
[15] S. Taki, T. Fujiwara, Numerical analysis of two-dimensional nonsteady detonations, AIAA J. 16 (1) (1978) 73–77.
[16] I.-wu Shen, T.C. Adamson, Theoretical Analysis of a Rotating Two Phase Detonation in a Rocket Motor, 1973, NASA CR 121194.
[17] J. Kinddracki, P. Walanski, Z. Gut, Experimental research on the rotating detonation in gaseous fuels-oxygen mixtures, Shock Waves 21 (2011) 75–84.
[18] R.N. Ibragimov, Oscillatory nature and dissipation of the internal waves energy spectrum in the deep ocean, Eur. Phys. J. Appl. Phys. 40 (2007) 315–334.
[19] R.N. Ibragimov, Generation of internal tides by an oscillating background flow along a corrugated slope, Phys. Scr. 78 (2008) 065801.
[20] T. Colin, et al., Long wave approximations for water waves, Arch. Ration. Mech. Anal. 178 (3) (2005) 373–410.
[21] P.K. Kundu, Fluid Mechanics, Academic Press, 1990.
[22] Choi, et al., A mathematical model for nonlinear waves due to moving disturbances in a basin of variable depth, J. Korean Soc. Costal. Ocean Eng. 5 (1993) 191–197.
[23] A. Ali, H. Kalisch, Reconstruction of the pressure in long-wave models with constant vorticity, Eur. J. Mech. B Fluids 37 (2013) 187–194.
[24] R.N. Ibragimov, H. Villasenor, Energy balance associated with a mixing process at the interface of a two-layer longitudinal atmospheric model, J. Fluids Eng. 136 (7) (2014) 071202.
[25] R.N. Ibragimov, Nonlinear viscous fluid patterns in a thin rotating spherical domain and applications, Phys. Fluids 23 (2011) 123102.
[26] A.P. Borluk, et al., Particle dynamics in the KdV approximation, Wave Motion 49 (2012) 691–709.
[27] Shingaki, et al., Numerical study on wave propagation in a low-rigidity elastic medium considering the effects of gravity, Wave Motion 51 (2014) 729–742.
[28] G.D. Roy, S.M. Frolov, A.A. Borisov, Pulse detonation propulsion: challenges, current status, and future perspective, Prog. Energy Combust. Sci. 30 (2004) 545.
[29] R.N. Ibragimov, M. Dameron, Group theoretical modeling of thermal explosion with reactant consumption, Commun. Nonlinear Sci. Numer. Simul. 7 (9) (2012) 3483–3489.
[30] N.H. Ibragimov, R.N. Ibragimov, Application of Lie group analysis to mathematical modeling in natural sciences, Math. Model. Nat. Phenom. 7 (2) (2012) 52–65.
[31] R. Zhou, J.P. Wang, Numerical investigation of flow particle paths and thermodynamic performance of continuously rotating detonation engines, Combust. Flame 159 (12) (2012) 3632–3645.